# Far-infrared spectra and associated dynamics in acetonitrile–water mixtures measured with femtosecond THz pulse spectroscopy

D. S. Venables and C. A. Schmuttenmaer
*Department of Chemistry, Yale University, 225 Prospect St., New Haven, Connecticut 06520-8107*

(Received 4 November 1997; accepted 22 December 1997)

We report the frequency-dependent absorption coefficient and index of refraction in the far-infrared region of the spectrum for mixtures of acetonitrile and water. The mixtures do not behave ideally, and deviate from ideality most noticeably for mixtures that are between 25% and 65% acetonitrile by volume. Two implementations of the Debye model for describing the dielectric relaxation behavior of mixtures are compared, and we show that these mixtures are better treated as uniform solutions rather than as two-component systems. We find an enhanced structure in the mixtures, relative to ideal mixtures, but we do not find direct evidence for microheterogeneity. The Debye time constant for the primary relaxation process for the mixtures is up to 25% longer than that for an ideal mixture. © *1998 American Institute of Physics.* [S0021-9606(98)52012-0]

## I. INTRODUCTION AND BACKGROUND

It is generally accepted that solvation and liquid dynamics are of fundamental importance.[1–4] The primary reason for the long-standing interest in this field is the large number of processes that occur in liquids and are significantly influenced by the surrounding solvent. For example, the solvent dynamics govern the solvation of protons, electrons, molecular ions, and neutral species. Charge transfer can also be influenced by the solvent dynamics.[5] The solvent affects the ease with which reactants approach, and products separate from, each other and thereby controls the rate and efficiency of many chemical reactions.[6,7] In addition, the solvent acts as a bath that can either supply thermal energy or accept excess energy, depending on the reaction. The underlying liquid dynamics are the common denominator for all these processes.

Although the dynamics of many pure liquids have been extensively investigated with both time domain and frequency domain experiments,[8–14] much less attention has been paid to mixtures of liquids, especially nondilute solutions and mixtures of highly polar liquids. The focus of studies of binary mixtures has often been on their deviation from ideal behavior. Usually, deviations from ideality are measured for thermodynamic mixing functions, although nonideal behavior of properties such as viscosity, heat capacity, and optical refractive index has also been investigated. Molecular dynamics (MD) simulations and spectroscopic techniques, especially Raman, infrared, far-infrared, microwave, and NMR spectroscopy, have also been valuable in elucidating the structure and dynamics of mixtures. In the work presented in this paper we will study the behavior of mixtures in the far-infrared region of the spectrum using femtosecond THz (fs-THz) pulse spectroscopy.

Mixtures of polar and nonpolar liquids are often studied in the far-infrared (FIR) by observing the behavior of the polar component.[15,16] This is possible because polar molecules, having a permanent dipole moment, absorb much more strongly than nonpolar ones, for which the only infrared-allowed absorption mechanism is collision-induced absorption. In this paper, however, we consider mixtures of water and acetonitrile, *both* of which are highly absorbing, polar liquids.

Water and acetonitrile are very important solvents, and water–acetonitrile mixtures find practical importance through their use in reversed-phase liquid chromatography.[17] The system has an upper critical solution temperature of 272 K at 0.38 mole fraction of acetonitrile, $x_{AN}$,[18] but the liquids are fully miscible over the entire range of compositions at temperatures above 272 K. The neat liquids each absorb strongly in the FIR below 1000 $cm^{-1}$, although their spectra are qualitatively somewhat different: acetonitrile has a peak at about 110 $cm^{-1}$, with a Napierian power absorption coefficient,[19,20] $\alpha$, of 600 per cm,[21] whereas $H_2O$ has a maximum Napierian power absorption of 3400 per cm near 700 $cm^{-1}$, and a shoulder of 1200 per cm at 200 $cm^{-1}$.[22]

One of the most fascinating aspects of mixtures of water with other liquids is the effect of the additional component on the water structure. For instance, small concentrations of nonpolar solutes tend to enhance the structure of water—this is the so-called ''iceberg'' hypothesis of Frank and Evans.[23] At intermediate compositions of water and nonelectrolyte, Naberukhin and Rogov proposed that the solute brought about the formation of regions of enhanced water structure (usually including some solute molecules) that are surrounded by a more disordered mixture of water and solute molecules.[24] They referred to this as ''microheterogeneity.'' The primary evidence for this suggestion was that both the enthalpies and entropies of mixing were negative at water-rich compositions. The only way to simultaneously justify the behavior of these thermodynamic quantities requires that the nonelectrolyte be accommodated in a more structured environment without breaking many water–water hydrogen bonds.

Questions of structure have been central to studies of mixtures of water and acetonitrile, and microheterogeneous behavior frequently has been assumed. As Fig. 1 shows, however, the thermodynamic behavior of water/acetonitrile

 

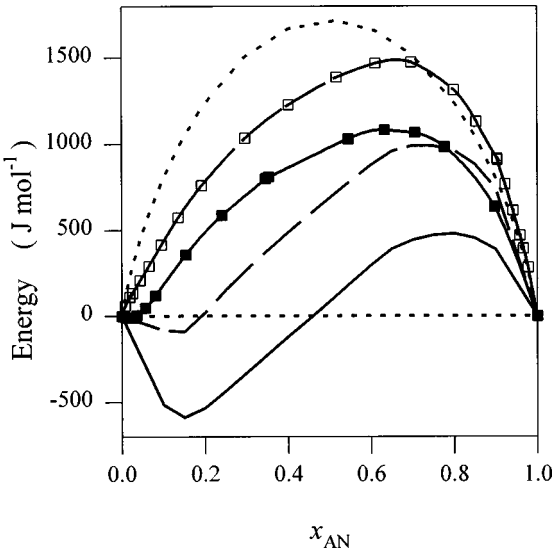


FIG. 1. Enthalpy and entropy of mixing for three aqueous mixtures as a function of the nonelectrolyte mole fraction. The dotted lines indicate an ideal mixture, for which $\Delta H_{\text{id mix}}=0$ and $T\Delta S_{\text{id mix}}=x_1 \ln x_1+x_2 \ln x_2$, where $x_1$ and $x_2$ are the mole fractions of each species. The solid line with the filled symbols is $\Delta H_{\text{mix}}$ for acetonitrile, and the dashed line with open symbols is $T\Delta S_{\text{mix}}$ for acetonitrile. The solid line without symbols is $\Delta H_{\text{mix}}$ and the dashed line without symbols is $T\Delta S_{\text{mix}}$ for water/dioxan, a more typical water/organic mixture (Ref. 25).

mixtures differs from that of other water and nonelectrolyte systems. In an ideal solution, the entropy increases due to the increased randomness rather than to a change in solution structure *per se*, and the enthalpy of mixing is zero, since the interactions of the dissimilar species are the average of the interactions of the two like species. In a typical water/organic mixture, at water-rich compositions the entropy of mixing is actually negative, as is the enthalpy. This unusual behavior has been attributed to microheterogeneity. However, the thermodynamics of mixing for water/acetonitrile are qualitatively different from those of other water/organic mixtures.[25] The entropy of mixing is never negative, and the enthalpy of mixing is positive, except for a small region where the mole fraction of acetonitrile is less than 0.04. These differences make the adoption of the microheterogeneity concept questionable for water and acetonitrile, and the unique thermodynamics of these mixtures is one of the reasons we wanted to study this system further. We wanted to see if there was any clear evidence of microheterogeneity or clustering in the FIR spectra. For example, would these clusters be well enough defined to produce distinct features in the spectra? And how would the dynamics of the system deviate from ideality?

There is a considerable, and often contradictory, body of work for the water/acetonitrile system. Thermodynamic properties of mixing have been reported in a number of papers.[18,26–36] Moreau and Dohéret examined the density, partial molar volumes of mixing, viscosity, and activation energy for viscous flow,[26] as well as the dielectric properties of the system.[27] They divided the system into three structural regions: for $x_{\text{AN}}<0.2$, acetonitrile molecules occupy voids in the water structure, with no enhancement of the water structure; for $0.2\leqslant x_{\text{AN}}\leqslant 0.8$, microheterogeneous behavior predominates with large aggregates formed; and for $x_{\text{AN}}>0.8$, the acetonitrile structure is disrupted by water. They did not regard acetonitrile as a strong breaker of water structure. The viscosity data generated by Moreau and Dohéret based on previous work by others[28] were also used in studies by Davis[29] and Easteal.[30] Regrettably, the primary data were not sufficient to reproduce accurately the viscosity at high acetonitrile concentrations (as Davis later pointed out[31]) so that some of the conclusions from these papers should be treated with caution. Apparent molar volumes and heat capacities in the mixtures have been reported by De Visser and co-workers,[32] who considered acetonitrile to be a structure breaker, owing either to intermolecular interactions, or to bulk diffusion which results in smaller water clusters. The Kirkwood–Buff integrals of the system have been calculated and indicate a strong tendency for each component to self-associate.[33] This effect was most pronounced between 0.3 and 0.4 mole fraction acetonitrile, and was attributed mainly to changes in the water structure.

Easteal studied the tracer diffusion coefficients of water and acetonitrile in the mixtures, and concluded that in mixtures containing 0.10 to 0.70 mole fraction acetonitrile the water exists in a more structured form than in the neat liquid.[30] Davis analyzed literature data of the excess volumes, enthalpies, and viscosities, as well as excess dielectric properties, in terms of a model based on three or four different structural compositions.[29,31,34,35] Based on his model, he inferred that the mobilities of both components decrease in the mixtures.

A number of spectroscopic studies of water and acetonitrile mixtures have been carried out.[37–43] Eaton and co-workers[37,38] used NMR and IR spectroscopy of the CN stretch to study the system. Their results suggest that acetonitrile accepts two hydrogen bonds from water, a conclusion borne out by their molecular dynamics simulations of a water-rich mixture. Jamroz *et al.*[39] and Bertie *et al.*[40] also used IR spectroscopy to study the CN and OD stretching bands of the mixtures. They concluded that molecules in the solution tended to associate with like species, although strong hydrogen bonds did form between acetonitrile and water. The water structure was slightly weakened, and dimers, trimers, and higher oligomers of water were formed. From a Raman study of the CN stretch, Rowlen and Harris believed that acetonitrile existed in two forms in the mixtures, neither of which involved hydrogen bonding.[40] Acetonitrile molecules interacted strongly with each other, even at low concentrations, and self-association was favored at acetonitrile-rich compositions. Stoev *et al.*[42] studied the CN stretch with both IR and Raman methods, and found that acetonitrile–water interactions were strongest near $x_{\text{AN}}=0.4$, and the amount of monomeric acetonitrile exceeded that of associated acetonitrile. The NMR work of Goldammer and Hertz[43] produced evidence of microheterogeneity in the mixtures based on reorientational time constants. Water–acetonitrile interactions were weak, although small amounts of acetonitrile led to an increase in the structure of the solution.

Perhaps the least ambiguous picture of the structure and dynamics of the system has been produced by computational work,[44–46] especially molecular dynamics simulations.[47,48]

The detailed MD simulations of Kovacs and Laaksonen[49] have been especially valuable in understanding the system. They studied the neat liquids and mixtures at acetonitrile mole fractions of 0.12, 0.50, and 0.88, and found an association of acetonitrile molecules over the whole composition range. Dimers, trimers, and tetramers of water were observed, and water structure was believed to be enhanced with the addition of acetonitrile. Water and acetonitrile formed hydrogen bonds, with stronger interactions at acetonitrile-rich compositions. Dynamical properties showed slower diffusion of both species at low acetonitrile compositions, which was attributed to an enhanced water structure. Larger diffusion coefficients were found at higher acetonitrile concentrations, owing to a breakdown of the water hydrogen-bonded network. An analysis of angular velocity time correlation functions suggested that small amounts of water disrupted acetonitrile dimerization. At high acetonitrile concentrations, water molecules gain motional freedom owing to fewer hydrogen bonds, in agreement with NMR correlation times. However, Hawlicka has pointed out that their assertion of water self-association is rendered inconclusive by the absence of coordination numbers and a hydrogen-bond analysis.[50]

## II. EXPERIMENT

Dielectric relaxation measurements of liquids and their mixtures have typically been carried out in the microwave region of the spectrum. This is because both the absorption coefficient, $\alpha = 4\pi\nu k/c$, and index of refraction, $n$, are needed to determine the frequency-dependent, complex dielectric function, $\hat{\epsilon}(\nu) = \epsilon'(\nu) - i\epsilon''(\nu)$ [where $\epsilon'(\nu) = n^2(\nu) - k^2(\nu)$, and $\epsilon''(\nu) = 2n(\nu)k(\nu)$, and $\nu$ is the frequency]. The absorption coefficient and index of refraction are readily measured simultaneously over a large range of frequencies with microwave technology. Recent technological advances in producing fs-THz pulses now allow both the absorption coefficient and index of refraction of a sample to be measured simultaneously at frequencies up to several hundred wave numbers.[51–55] Using this technique, we report both the absorption coefficient and index of refraction for these mixtures from 3 to 55 $cm^{-1}$.

Mixtures were made from deionized water, and from acetonitrile obtained from Baker (99.6% pure). The volumes required to make up the desired composition were measured with a calibrated pipette, and were chosen to yield a total volume for the mixture of 25–30 mL. The uncertainty in the volume of each component was less than 0.05 mL, giving an uncertainty of less than 0.2% in the volume fraction.

The fs THz pulse spectrometer used is shown in Fig. 2, and is essentially the same as that described previously.[51,52] One notable change to the spectrometer is the addition of a photodiode, which was used to monitor the power of the optical beam. The THz pulse amplitude was found to be linearly dependent on the optical power for variations less than 10%, thereby permitting fluctuations in the power of the optical pulse to be accounted for during data collection. As before, the sample was held in a polyethylene bag sandwiched between two high-resistivity Si windows, one of which was mounted on a translation stage. For most compositions, the pathlength of the THz pulse was varied manually by adjusting a micrometer on the translation stage. However, for two of the compositions, an automated pathlength adjustment procedure was implemented. The translation stage was driven by a DC motor micrometer and the distance moved was determined using a calibrated linear voltage to distance transducer (LVDT). The precision was about $\pm 1$ $\mu$m for either method of varying the pathlength. The experiments were carried out at room temperature 18 °C–20 °C, and the THz system was enclosed in a box and flushed with dry nitrogen to reduce absorption from water vapor. Time domain spectra were recorded over 50.13 ps with a time step of 48.96 fs (1024 data points per scan), and 30 scans were averaged for each pathlength. Seven pathlengths were used, ranging from 30 to 200 $\mu$m. The data were processed in the same manner as that described earlier.[52] Five to eight data sets were measured for each mixture.

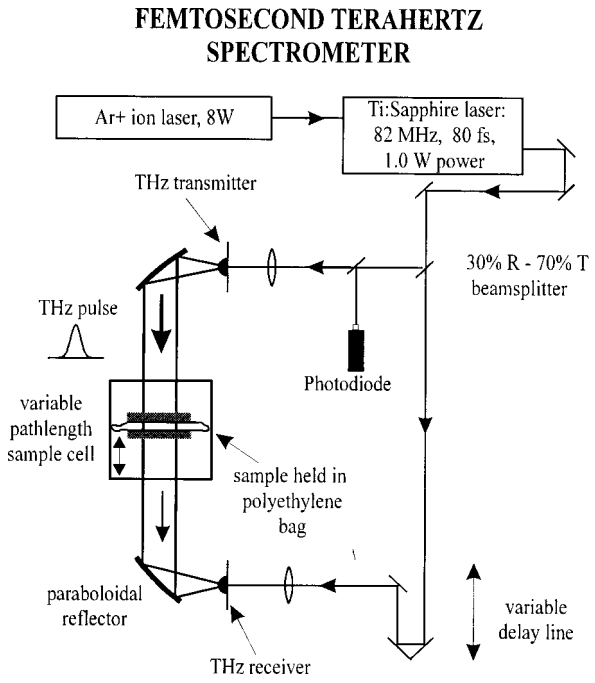


FIG. 2. A schematic representation of the experimental apparatus. Subpicosecond far-infrared pulses (often referred to as fs-THz pulses) are generated at the transmitter by ultrafast photoexcitation of a biased semiconductor wafer using a Ti:Sapphire laser. After passing through the sample cell, the pulses are synchronously detected at the receiver with a portion of the visible laser pulse. The time-dependent electric field of the THz pulse is determined by varying the optical delay between the visible pulses driving the transmitter and receiver.

## III. RESULTS

Spectra of seven mixtures of $CH_3CN$ and $H_2O$ were measured along with spectra of the two neat liquids. The mixtures contained 90%, 75%, 65%, 50%, 35%, 25%, and 10% $CH_3CN$ by volume before mixing. The reasons that the analysis is in terms of volume fraction rather than mole fraction are discussed in Sec. IV A. The absorption coefficients and indices of refraction as a function of frequency for the 0%, 25%, 50%, 75%, and 100% acetonitrile mixtures are shown in Fig. 3. At high frequencies, we note the relatively smooth trend of increasing absorption coefficient, and de-

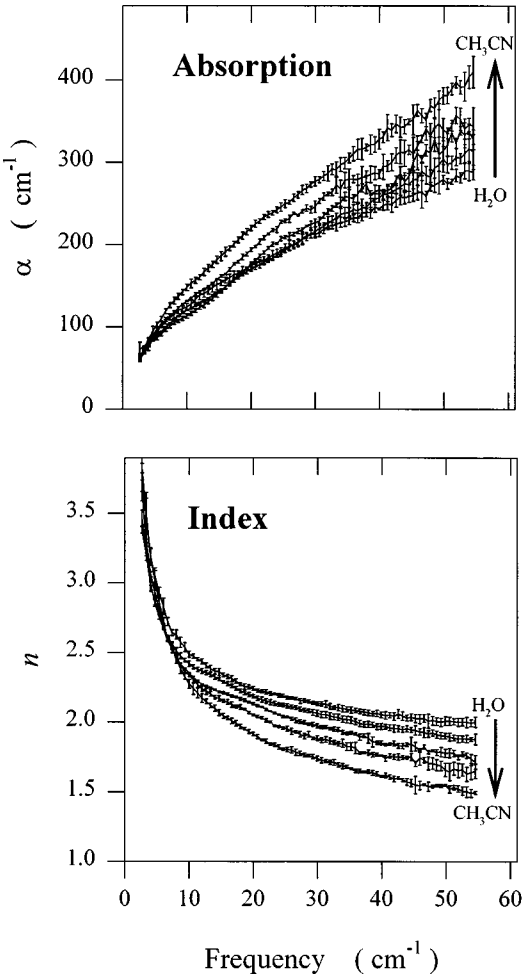


FIG. 3. Absorption coefficient and index of refraction from 3 to 55 $cm^{-1}$ for neat water, neat acetonitrile, and mixtures that are 25%, 50%, and 75% acetonitrile by volume. The general trend is that the absorption coefficient increases, while the index of refraction decreases, as a function of increasing the acetonitrile fraction.

creasing index of refraction, as the $CH_3CN$ concentration increases. At lower frequencies, there are clearly some deviations from this smooth behavior. We do not find any distinct features in the mixtures that could be attributed to clusters, however.

Figure 4 displays $\alpha$ and $n$ as a function of acetonitrile volume fraction for several frequencies. The frequencies chosen are 5, 10, 15, 20, and 25 $cm^{-1}$. Higher frequencies are not shown, because in those cases the absorption coefficient and index of refraction behave essentially ideally. In general, the deviation of $\alpha$ from ideality starts at zero, increases in magnitude, and then returns to zero with increasing $CH_3CN$ fraction. The behavior of the index of refraction versus the volume fraction at various frequencies is interesting. For the lowest frequency shown, 5 $cm^{-1}$, it has large negative deviations, at 10 $cm^{-1}$ it behaves nearly ideally, and finally, at higher frequencies it behaves essentially ideally. Rather than attempt to interpret this behavior, we note instead that both the absorption coefficient and index of refraction contribute to the complex dielectric constant, which in turn is used to describe the dynamics of the liquid. As Fig. 5 shows, the deviations from ideality of the fitted parameters

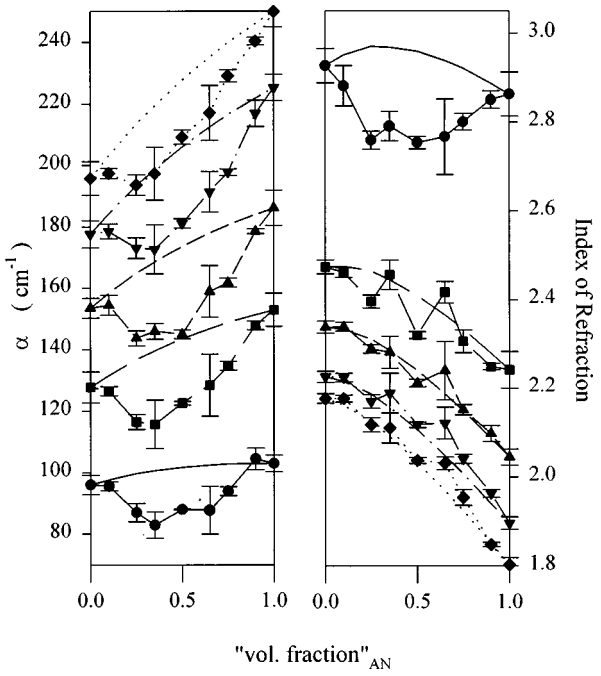


FIG. 4. The absorption coefficient and index of refraction as a function of *volume fraction* of acetonitrile at several frequencies. The frequencies chosen are 5, 10, 15, 20, and 25 $cm^{-1}$, and are indicated by circles, squares, triangles, inverted triangles, and diamonds, respectively. The smooth lines connecting the points for the neat liquids at $x_{AN}=0.0$ and $x_{AN}=1.0$ represent the expected behavior for an ideal mixture [see Eqs. (1) and (2)].

vary smoothly, and the behavior of the index of refraction at these frequencies should not be over-analyzed.

The 90%–10% and 10%–90% mixtures behave nearly ideally at all frequencies; that is, the deviation from ideality of both $\alpha$ and $n$ is small. We do not see behavior where the quantity has a positive deviation from ideality over one range of compositions, and a negative deviation over another range, as has been observed for excess properties such as entropy and enthalpy for other water/nonelectrolyte mixtures.[24]

Two different models were used to fit the data and will be described and compared in Sec. IV C. In brief, the single component, double Debye model proved superior to the two-component model based on the volume fraction-weighted spectra of the neat liquids. The parameters of the double Debye model are plotted in Fig. 5, and listed in Table I. The static relative permittivity, $\epsilon_0$, for each mixture was held fixed during the fitting procedure,[56] but the values are shown for completeness. The results of the fits are not highly dependent on the value of the static dielectric constant. Variations of 2%–3% do not affect the results. In Fig. 5, the solid lines indicate the expected behavior for an ideal mixture. The large filled circles with error bars are the mean and $1\sigma$ standard deviation for the fitted parameters as a function of acetonitrile volume fraction. These are the values given in Table I.

## IV. DISCUSSION

### A. Volume fractions

The properties of binary mixtures are usually described as a function of mole fractions of the constituent species, but

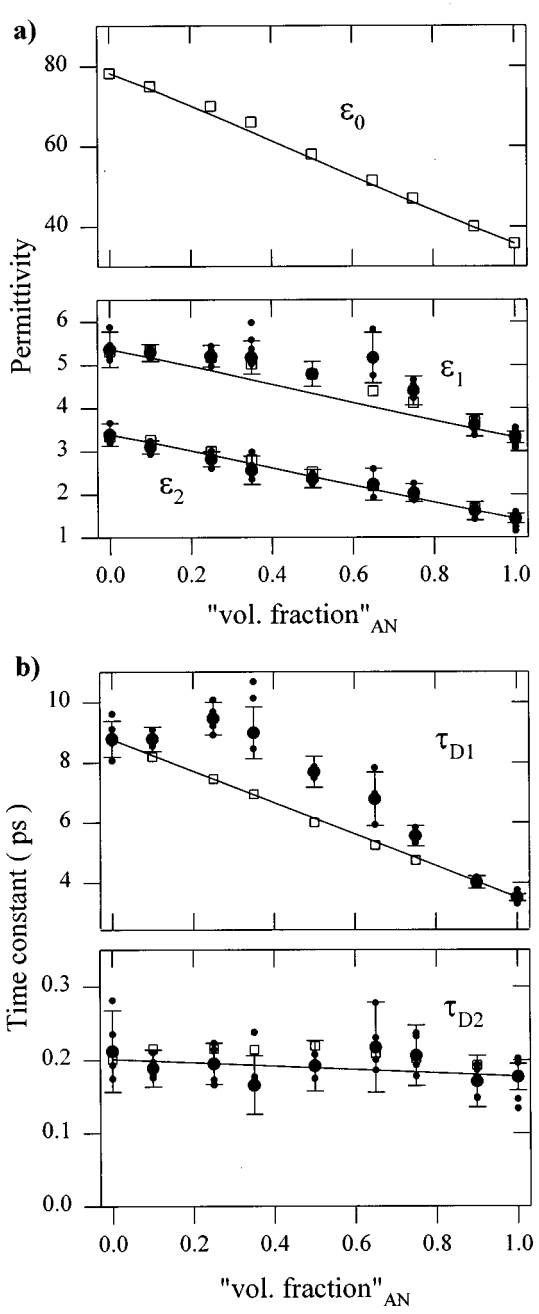


FIG. 5. The results of fitting a double Debye model to the measured data. The numerical values of the parameters plotted here are given in Table I. Part (a) shows the static and high-frequency permittivity as a function of the acetonitrile volume fraction, and part (b) shows the Debye relaxation time constants for the two processes, also as a function of volume fraction. The large filled circles with error bars represent the fitted parameters and $1\sigma$ uncertainty. The solid lines represent an ideal mixture. The open squares represent the results of fitting the double Debye model to an ideal dataset generated by combining the absorption coefficient and index of refraction of the two neat liquids based on their volume fractions using Eqs. (1) and (2). The faster Debye process characterized by $\tau_{D2}$ and $\epsilon_2$ behaves essentially ideally, but the slower process characterized by $\tau_{D1}$ and $\epsilon_1$ shows significant deviations from ideality. The relaxation time constant for the actual mixture is roughly 25% longer than for an ideal mixture when the acetonitrile volume fraction is between 25% and 65%.

we choose to use the volume fraction for a number of reasons. In the first place, the power absorption coefficient is the reciprocal of the distance through which the transmitted power falls to $1/e$ of its incident value. If a sample cell contains a mixture of two liquids, and there is no change in partial molar volume of the liquids upon mixing, then the measured absorption would be identical to that obtained with a membrane separating the sample cell into two volumes that are proportional to the volume fraction of each species in the mixture (assuming reflections at the interface are negligible). That is, the effective pathlength for each species is determined by its volume fraction. On the other hand, if an experiment measures a chromophore that is dissolved in a solvent at relatively small concentrations, then the mole fraction is an appropriate measure of concentration. The importance of using volume fractions in nondilute mixtures has been recognized previously.[57] Finally, we note that none of the interpretations or conclusions presented in this paper would be changed by using a mole fraction instead of a volume fraction. Doing so merely distorts the horizontal axis of the plots by compressing everything toward the left, since a 1:1 volume ratio for acetonitrile:water approximately corresponds to a 1:3 mole ratio (the molar volume for water is $18.1\ \mathrm{cm^3\ mol^{-1}}$, while that for acetonitrile is $52.5\ \mathrm{cm^3\ mol^{-1}}$).

### B. Ideal mixtures

It is not trivial to know what the value of any particular *non*-thermodynamic quantity should be for an ideal mixture.[35] For the purpose of this paper, we state that the absorption coefficient and index of refraction of an ideal mixture would have the volume-weighted absorption coefficient and index of refraction of the constituent species. If the density of the mixture is greater or less than that calculated from the volume fraction-weighted mixture, then $\alpha$ and $n$ should increase or decrease accordingly. For mixtures of acetonitrile and water, the total volume is slightly less than the sum of the two volumes mixed. The increase in density only amounts to about 2.3% at its greatest deviation, obtained with a 50%–50% mixture.[58] The reduction in total volume is due to the packing of objects of dissimilar sizes. In extreme cases, smaller objects can fit completely into the crevices between the larger objects, which results in a large decrease in the total volume compared to the sum of the volumes of the objects before mixing. The volume of a $CH_3CN$ molecule is a factor of 2.9 times greater than that for a $H_2O$ molecule, which results in only a minor decrease in the total volume due to packing. We use the formula from Ref. 57 for the absorption coefficient of the ideal mixture,

$$\alpha_{\mathrm{ideal}}(\nu)=a_1\alpha_1(\nu)+a_2\alpha_2(\nu), \tag{1}$$

where $\alpha_i$ is the absorption coefficient for each species, and the coefficient $a_i=C_i^{\mathrm{mix}}/C_i^{\mathrm{neat}}$ is the concentration of species $i$ in the mixture divided by its concentration in the pure liquid. For a mixture in which $\Delta V_{\mathrm{mix}}=0$, the coefficients $a_i$ reduce to the volume fraction of each species. Similarly, we define the ideal index of refraction, $n_{\mathrm{ideal}}$, to be

$$n_{\mathrm{ideal}}(\nu)=a_1n_1(\nu)+a_2n_2(\nu), \tag{2}$$

where $n_i$ is the index of refraction for each species.

The ideal spectrum is exactly the same spectrum that would be obtained if the probe beam went through two sepa-

TABLE I. Fitted parameters with $1\sigma$ uncertainties (in parentheses) for mixtures of acetonitrile and water using a double Debye model.

| $a_{ACN}$ | $\epsilon_s$ | $\epsilon_1$ | $\epsilon_2$ | $\tau_{D1}$ | $\tau_{D2}$ |
|---|---|---|---|---|---|
| 0.000 | 78.300 | 5.370 (0.408) | 3.392 (0.262) | 8.794 (0.595) | 0.212 (0.055) |
| 0.100 | 75.000 | 5.290 (0.195) | 3.100 (0.152) | 8.780 (0.408) | 0.189 (0.025) |
| 0.250 | 70.000 | 5.210 (0.251) | 2.820 (0.175) | 9.460 (0.540) | 0.195 (0.028) |
| 0.350 | 66.000 | 5.173 (0.386) | 2.561 (0.329) | 8.990 (0.860) | 0.166 (0.040) |
| 0.500 | 58.000 | 4.790 (0.293) | 2.360 (0.211) | 7.690 (0.511) | 0.192 (0.034) |
| 0.650 | 51.500 | 5.165 (0.589) | 2.228 (0.367) | 6.780 (0.893) | 0.217 (0.061) |
| 0.750 | 47.000 | 4.400 (0.333) | 2.030 (0.205) | 5.550 (0.338) | 0.206 (0.041) |
| 0.900 | 40.000 | 3.600 (0.254) | 1.610 (0.214) | 4.010 (0.208) | 0.171 (0.035) |
| 1.000 | 35.770 | 3.323 (0.137) | 1.439 (0.108) | 3.506 (0.114) | 0.177 (0.018) |

rate sample cells in succession (disregarding any reflection losses at the interface), or if it went through a sample cell containing two completely immiscible liquids with the same index of refraction. How then is it possible to distinguish among a true mixture, a microheterogeneous mixture, and two separate liquids? We relied on the results of fitting the measured data to two different implementations of the Debye model, and selected the one that was most consistent in describing all of the measured data. If a mixture behaves ideally, then it is impossible to distinguish among these possibilities. Acetonitrile/water mixtures do not behave ideally, however, and this allows us to determine the best implementation of the Debye model.

### C. Competing models

The choice of model for extracting dynamical information is very important in this study, since these measurements, although made in the time domain, only yield frequency domain information. One of the most commonly used models to describe dielectric relaxation is the Debye model, which describes the dynamics in terms of collective, diffusive, reorientational motions in the liquid. The model is most easily understood in the context of the decay of the induced polarization that would occur in a dipolar liquid if an applied static electric field were instantaneously turned off: the polarization of the sample would decay exponentially. The time constant for the decay is referred to as the Debye time, $\tau_D$, and is determined from the experimental data as the reciprocal of the frequency (in radians per second) that corresponds to the maximum value of the dielectric loss ($\epsilon''$).

Microwave data are sensitive to collective diffusive motions in the liquids that occur on a time scale of several picoseconds to hundreds of nanoseconds. Many of the processes occurring in liquids are faster than this, which implies that measurements must be made at higher frequencies. The FIR region of the spectrum is sensitive to faster processes: for example, the period corresponding to $33.3\,cm^{-1}$, or 1 THz, is 1 ps. Although the Debye model breaks down when the motions that occur at a given frequency change from being collective and diffusive to intermolecular and damped oscillatory, it is still important that the period of the probe radiation match the time scale of the dynamics.

The real and imaginary components of the frequency-dependent permittivity are described by the Debye model as[14]

$$\hat{\epsilon}(\omega)=\epsilon_\infty+\sum_{j=1}^{n}\frac{\epsilon_j-\epsilon_{j+1}}{1+i\omega\tau_{Dj}}. \tag{3}$$

Here, $\omega$ is the angular frequency, $\epsilon_1$ is the static dielectric constant, $\epsilon_j$ are intermediate steps in the dielectric constant, $\epsilon_{n+1}=\epsilon_\infty$ is its limiting value at high frequency, and $n$ is the number of relaxation processes, each of which has a characteristic time constant, $\tau_{Dj}$. The Debye treatment with $n=1$ is the simplest case, and requires that a single relaxation time provide an adequate description. In this case, the expression for $\hat{\epsilon}(\omega)$ from Eq. (3) simplifies to[14]

$$\hat{\epsilon}(\omega)=\epsilon_\infty+\frac{\epsilon_s-\epsilon_\infty}{1+i\omega\tau_D}, \tag{4}$$

and it is easy to separate the real and imaginary components:[14]

$$\epsilon'(\omega)=\epsilon_\infty+\frac{\epsilon_s-\epsilon_\infty}{1+\omega^2\tau_D^2} \tag{5}$$

and

$$\epsilon''(\omega)=\frac{(\epsilon_s-\epsilon_\infty)\omega\tau_D}{1+\omega^2\tau_D^2}. \tag{6}$$

Similar expressions are obtained for multiple Debye processes. The exponential decay time constant of the induced polarization is denoted $\tau_D$, and the magnitude of the induced polarization is given by the dispersion amplitude, $\Delta\epsilon=\epsilon_s-\epsilon_\infty$, where $\epsilon_s$ is the static dielectric constant and $\epsilon_\infty$ is the infinite frequency dielectric constant. Infinite frequency is attained when the oscillating electromagnetic field is far too rapid for the molecular framework to follow; that is, $n_{opt}=\sqrt{\epsilon_\infty}$, where $n_{opt}$ is the index of refraction at optical frequencies. If the decay of the induced polarization is a double exponential representing two independent processes, then there will be two Debye time constants, $\tau_{D1}$ and $\tau_{D2}$, and two dispersion amplitudes, $\Delta\epsilon_1$ and $\Delta\epsilon_2$. There are more refined treatments that explicitly allow for a distribution of relaxation time constants, either symmetrically or unsymmetrically distributed about a mean value, and are referred to as the Cole–Cole or Cole–Davidson models, respectively.

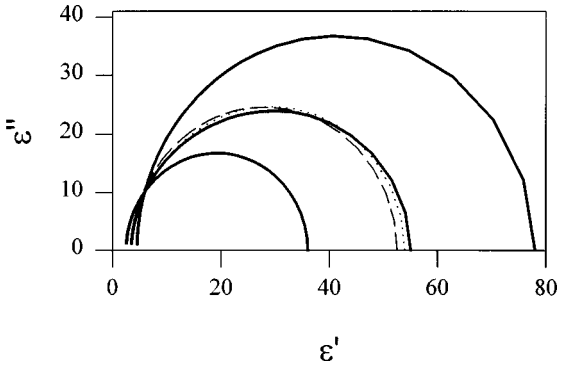


FIG. 6. The thick lines depict Cole–Cole plots for two single Debye liquids (the largest and smallest semicircles) and their ideal mixture (the thick intermediate curve). The thin dashed and dotted lines are the best fit of single and double Debye processes to the ideal mixture. The result of a fit based on the Debye parameters of the two neat liquids, wherein only the volume fraction is varied, is entirely superimposed on the intermediate thick solid line for the ideal mixture.

As the results of this paper do not depend on these more refined treatments, we will employ the Debye model to make the discussion more transparent.

We performed fits of $n(\nu)$ and $k(\nu)$ for all of the compositions using two different implementations of the Debye model. We found that treating the mixtures as true mixtures, i.e., not as a two-component heterogeneous solution, successfully fit the data for all of the compositions studied. Ultimately, we fitted the measured data for each of the mixtures to a double Debye model and compared the resulting parameters to those for the neat liquids. This is the most often used method,[14,59] and the results are shown in Fig. 5 and Table I.

The other implementation of the Debye model considered here was to treat the mixtures as being comprised of two noninteracting components that have the characteristics of the two pure liquids. This is an extreme case of microheterogeneity. A comparison of how well an ideal mixture is described by the two competing models is shown in Fig. 6, and is presented more quantitatively in Table II.

Consider a *simulated ideal* 50%–50% mixture of two neat liquids, $A$ and $B$, each of which is described by a single Debye process with parameters similar to those of acetonitrile and water. Table II shows the parameters describing each neat liquid, a simple average of the parameters, and the parameters obtained from a fit using both a single Debye model and a double Debye model. The thick lines in Fig. 6 show the Cole–Cole plots for two ideal liquids, each characterized by a single Debye process (the small and large semicircles), as well as that of a plot of an ideal 50%–50% mixture (the thick intermediate curve). A Cole–Cole plot is obtained by plotting $\epsilon''$ vs $\epsilon'$, and has the form of a semicircle for a single Debye process. The thin lines correspond to the results of nonlinear, least squares fits to the simulated ideal mixture based on single and double Debye models. The long dashed line in Fig. 6 is the best fit of the simulated mixture when using a single Debye process, and the dotted line is the best fit when using a two Debye process. The second implementation of the Debye model, in which the Debye parameters for the two pure liquids are fixed and only the volume fraction is varied, results in a fit that is superimposed on the intermediate thick solid curve, and is therefore not visible in the figure. Neither a single nor a double Debye fit to the mixture can accurately reproduce the noiseless simulated data.

TABLE II. Debye parameters for two neat liquids, $A$ and $B$, the mean values, and the best fits based on single and double Debye models.

| Liquid | $\epsilon_s$ | $\epsilon_1$ | $\epsilon_\infty$ | $\tau_{D1}$ | $\tau_{D2}$ |
|---|---|---|---|---|---|
| $A$ | 78 | ⋯ | 4.5 | 9 | ⋯ |
| $B$ | 36 | ⋯ | 2.5 | 3.5 | ⋯ |
| ''$(A+B)/2$'' | 57 | ⋯ | 3.5 | 6.25 | ⋯ |
| $A+B$, single Debye | 52.6 | ⋯ | 3.47 | 5.5 | ⋯ |
| $A+B$, double Debye | 54.0 | 5.59 | 3.44 | 6.4 | 1.4 |

Table II presents these findings in a more quantitative fashion. The single Debye fit of the simulated ideal mixture reproduces the value of the infinite frequency permittivity, $\epsilon_\infty$, but not the static permittivity, $\epsilon_s$, or relaxation time constant, $\tau_{D1}$. The double Debye fit performs somewhat better in reproducing $\epsilon_s$, $\epsilon_\infty$, and $\tau_{D1}$, but the values obtained for the intermediate permittivity, $\epsilon_1$, and the second relaxation time constant, $\tau_{D2}$, do not bear an obvious relationship to the parameters of the species $A$ and $B$ that make up this simulated ideal mixture. That is, there are now too many variable parameters in the fit. In summary, an ideal mixture will not necessarily be properly described by the Debye model as a single component because if the unlike species do not interact with each other at all, then the decay of the induced polarization of one species will not be affected by the presence of the other.

While the above implementation based on two components in a microheterogeneous mixture is the appropriate way to describe the simulated ideal mixture, we could not use it to successfully fit all the measured data unless parameters were allowed to vary in ways that were not physically meaningful. Our goal when using this implementation was to fit the measured data by only varying the volume fraction of each component, while holding the Debye parameters fixed at their known values for the neat liquids. The static permittivity for each component of the mixture was held fixed at the experimental value for the mixture, rather than at the static value for the neat liquid. We found that reasonable fits could only be obtained if the Debye relaxation time constant, $\tau_{D1}$, for the slower process for each neat liquid was not held fixed during the fit. Furthermore, the fitted values of $\tau_{D1}$ did not vary smoothly as a function of composition, and the volume fractions obtained for each component differed by as much as 8% from the known composition.

In order to rule out possible artifacts of the implementation chosen (a single-component, double Debye model), we performed two checks. We first verified that the model was not over-parametrized, and we then verified that the model could distinguish between the real data sets and an ideal data set based on the spectra of the neat liquids. Five or more data sets were averaged together before performing the fits, which yields the $1\sigma$ error bars shown in Fig. 3. The small filled circles without error bars in Fig. 5 represent the parameters obtained when performing the fits when using values

for $\alpha$ and $n$ that are $1\sigma$ greater or less than their mean value. There are four possible $\alpha$, $n$ combinations: $\bar{\alpha}+1\sigma,\bar{n}+1\sigma$; $\bar{\alpha}+1\sigma,\bar{n}-1\sigma$; $\bar{\alpha}-1\sigma,\bar{n}+1\sigma$; and $\bar{\alpha}-1\sigma,\bar{n}-1\sigma$. The fact that the parameters obtained in this method are almost always within the error bars of the parameters when fitting the mean values of $\alpha$ and $n$ indicates that the model is not over-parametrized. The open squares represent the parameters obtained when fitting the model to ideal-mixture data sets generated by calculating the volume-weighted fraction of $\alpha$ and $n$ for the neat liquids using Eqs. (1) and (2). These points fall quite close to the solid line of ideality, which indicates that the model will yield different results for ideal mixtures, and that the deviations from ideality for the actual mixtures are significant and not an artifact of the fitting procedure. Since the open squares are outside the error bars of our actual fits, and the two-component model could not successfully fit the measured data, we assert that the mixtures behave as a single component, not micro-multicomponent, on the length scale probed by FIR radiation.

### D. Dynamics and structure

The parameters describing the neat liquids and their mixtures are plotted in Fig. 5 and presented in Table I. The static relative permittivity[56] for each mixture was held fixed during the fitting procedure. The results for pure water are within the uncertainty of the values we reported previously.[52] There is a process with an 8.8 ps time constant that is attributed to collective reorientation, and a faster process that is attributed to hydrogen bond formation and breaking.[14] The results for pure acetonitrile are in good agreement with the literature values[14] when it is taken into account that previous reports only measured the complex dielectric function up to 89 GHz. In that case, a single process with a 3.48 ps time constant suffices to fit the measurements. We must include a second process with a 0.18 ps time constant to fit the data that extends to 55 $cm^{-1}$ (1.65 THz). The slower process is attributed to collective reorientation, and the faster process might be due to the formation and breaking of cyclic dimer structures. The amount of dipolar alignment, either end-on-end or cyclic antiparallel, is quantified by the value of the Kirkwood $g$ factor.[60] The Kirkwood $g$ factor of acetonitrile is roughly 0.45, based on Eq. (1) of Ref. 60, which indicates the presence of antiparallel dipoles, since a value of less than unity arises when the constituent molecules pair up in an antiparallel fashion and thereby partially cancel out the net dipole moment.

The relative amount of low-frequency FIR absorption of a liquid depends inversely on its amount of structure. For example, in the case of pure water, where the structure is due to hydrogen bonding, it is known that the degree of hydrogen bonding, and hence the structure, decreases as the temperature is raised.[61–63] Infrared and Raman studies show that the hydrogen bonded to nonhydrogen bonded band intensity ratio for the OH (or OD) stretch decreases with increasing temperature.[61] The effect of hydrogen bond breaking on the FIR spectrum depends on the type of motion involved. Typically, at frequencies greater than about 600 $cm^{-1}$, the intensities of librational bands caused by oscillatory motions decrease[64] since these modes depend on the tetrahedral moiety remaining intact. At lower frequencies, where the absorption arises from orientational or translational diffusional modes, the absorption intensity increases[54,64] as these motions become more facile. Indeed, the Debye relaxation time constant for pure water decreases with increasing temperature,[54,65] indicating a decrease in structure. The point here is not simply that the structure decreases with increasing temperature, but rather that the low-frequency FIR absorption increases as the structure decreases, regardless of temperature. Thus, the observed decrease in absorption for the water/acetonitrile mixtures relative to ideal mixtures shown in Fig. 4 is attributed to an increase in the overall structure of the liquid, relative to ideal. It is especially pronounced when the volume fraction is between 25% and 65%. The decrease in absorption coefficient cannot be explained by the nonideal volume of mixing, because the increase in density would predict a stronger, not weaker, absorption.

The increase in structure is manifested by the increased value of the Debye relaxation time constant of the slower process, $\tau_{D1}$, relative to ideality. A larger value of $\tau$ indicates that the molecules respond more slowly to an oscillating field, as would be expected for more structured liquids. This indicates that the collective intermolecular modes are strongly affected in the mixtures. The relaxation time constant increases by as much as 25% for mixtures that are 25% to 35% acetonitrile by volume. The increase in relaxation time constant is consistent with the observed decrease in the absorption coefficient compared to the ideal case, and both are consistent with an increase in the structure of the liquid.

As discussed in the Introduction, previous studies based on a wide variety of experimental techniques have inferred the presence of microheterogeneous regions, or clusters, within mixtures of $CH_3CN$ and $H_2O$. The thermodynamics of water/acetonitrile mixtures are somewhat different than those for other water/nonelectrolyte mixtures, however. In cases where microheterogeneity occurs, the thermodynamic mixing functions show minima and maxima, which is not observed in water/acetonitrile mixtures. We conclude that there is indeed an enhanced structure of the mixtures relative to the neat liquids, but that there is not microheterogeneity, or if there is, it is not manifested in the low-frequency absorption spectra. There are no new features at a given composition, or a spectrum for a particular composition that displays a significant qualitative difference from the others, indicating distinct globular entities. Furthermore, fitting the data as a two-component liquid did not give meaningful results.

In a microheterogeneous mixture, the measured dynamics will depend on the length scale of interaction. If the interaction distance is greater than the dimensions of several molecules, then one would expect a Debye time constant and dispersion amplitude for the mixture that is different from either neat component. However, if the interaction distance is very small, then it would be more appropriate to describe the mixture as containing two components: each neat liquid, perhaps with slightly modified parameters due to interfacial effects.

## V. CONCLUSIONS

The dynamics of mixtures of two highly polar molecules, $H_2O$ and $CH_3CN$, have been measured and found to behave nonideally. While the observation that a mixture of two highly polar molecules behaves nonideally is fairly obvious, we have sought to quantify the nonideality of the time scale of reorientation, which is not so obvious. The mixtures exhibit more structure than an ideal mixture, based on the increase in the relaxation time constant and a decrease in the absorption coefficient, relative to an ideal mixture. After considering two possible implementations of the Debye model of dielectric relaxation, we find that the mixtures are best described as not having microheterogeneity. Furthermore, no distinct spectral features were observed that would indicate the presence of well-defined clusters or globules in the mixtures.

Several future studies will provide additional insight into water/organic mixtures. Obtaining the spectra of the mixtures to higher frequency will certainly be useful. A temperature-dependent study, at both higher and lower temperatures, would be very interesting, especially as the mixture is cooled near its upper critical temperature (272 K, $x_{AN}=0.38$). Two related mixtures will also be studied. Methanol/water mixtures will be informative for several reasons: $CH_3OH$ can both donate and accept hydrogen bonds, unlike $CH_3CN$, which can only accept them, but otherwise the molecules are similar in size and static permittivity. Acetone/water mixtures would be interesting because the thermodynamic properties show more promise of microheterogeneity, yet $CH_3COCH_3$, like $CH_3CN$, can only accept hydrogen bonds.

## ACKNOWLEDGMENTS

This work was partially supported by the Camille and Henry Dreyfus Foundation New Faculty Award Program. Acknowledgment is also made to the donors of The Petroleum Research Fund, administered by the ACS, for partial support of this research.

[1] I. Rips, J. Klafter, and J. Jortner, J. Chem. Phys. **88**, 3246 (1988).
[2] F. O. Raineri, H. Resat, B. C. Perng, F. Hirata, and H. L. Friedman, J. Chem. Phys. **100**, 1477 (1994).
[3] B. Bagchi and A. Chandra, Adv. Chem. Phys. **80**, 1 (1991).
[4] M. Maroncelli, J. Mol. Liq. **57**, 1 (1993).
[5] R. A. Marcus, Pure Appl. Chem. **69**, 13 (1997).
[6] Z. B. Alfassi, R. E. Huie, and P. Neta, J. Phys. Chem. **97**, 7253 (1993).
[7] I. H. Um, G. J. Lee, H. W. Yoon, and D. S. Kwon, Tet. Lett. **33**, 2023 (1992).
[8] P. Vöhringer and N. F. Scherer, J. Phys. Chem. **99**, 2684 (1995).
[9] Y. J. Chang and E. W. Castner, Jr., J. Phys. Chem. **100**, 3330 (1996).
[10] S. Kinoshita, Y. Kai, M. Yamaguchi, and T. Yagi, Phys. Rev. Lett. **75**, 148 (1995).
[11] S. Palese, J. T. Buontempo, L. Schilling, W. T. Lotshaw, Y. Tanimura, S. Mukamel, and R. J. D. Miller, J. Phys. Chem. **98**, 12 466 (1994).
[12] T. Lian, Y. Kholodenko, and R. M. Hochstrasser, J. Phys. Chem. **99**, 2546 (1995).
[13] M. Cho, M. Du, N. F. Scherer, G. R. Fleming, and S. Mukamel, J. Chem. Phys. **99**, 2410 (1993).
[14] J. Barthel and R. Buchner, Pure Appl. Chem. **63**, 1473 (1991).
[15] E. Knözinger, D. Leutloff, and R. Wittenbeck, J. Mol. Struct. **60**, 115 (1980).
[16] T. Tassaing, Y. Danten, M. Besnard, E. Zoidis, J. Yarwood, Y. Guissani, and B. Guillot, Mol. Phys. **84**, 769 (1995).
[17] Y. C. Guillaume and C. Guinchard, Anal. Chem. **69**, 183 (1997).
[18] D. A. Armitage, M. J. Blandamer, M. J. Foster, N. J. Hidden, K. W. Morcom, M. C. R. Symons, and M. J. Wooten, Trans. Faraday Soc. **67**, 1193 (1968).
[19] The Napierian power absorption coefficient, $\alpha$, is based on Beer's law: $P/P_0=e^{-\alpha d}$, where $P_0$ is incident power, $P$ is transmitted power, and $d$ is the sample thickness in cm. Upon rearrangement, we find $\alpha=[\ln(P/P_0)]/d$, and this is the quantity plotted in Figs. 3 and 4. Unfortunately, $\alpha$ is often incorrectly reported with units of ''neper/cm,'' which can cause confusion. One neper (1 Np) is the level of a field, or *amplitude*, quantity when $F/F_0=e$ (where $e$ is the base of natural logarithms) or equivalently, $\ln(F/F_0)=1$.[20] Therefore, it is the level of a power, or intensity, quantity when $P/P_0=e^2$, or $\ln(P/P_0)=2$, *not* when $\ln(P/P_0)=1$, as is often incorrectly assumed.
[20] B. N. Taylor, *Guide for the Use of the International System of Units (SI)*, NIST Special Publication 811, 1995 edition (U.S. Government Printing Office, Washington, DC, 1995).
[21] T. Ohba and S. Ikawa, Mol. Phys. **73**, 985 (1991).
[22] J. E. Bertie and Z. D. Lan, Appl. Spectrosc. **50**, 1047 (1996).
[23] H. S. Frank and M. W. Evans, J. Chem. Phys. **13**, 507 (1945).
[24] Y. I. Naberukhin and A. Rogov, Russ. Chem. Rev. **40**, 297 (1971).
[25] H. T. French, J. Chem. Thermodyn. **19**, 1155 (1987); K. W. Morcom and R. W. Smith, *ibid.* **1**, 503 (1969).
[26] C. Moreau and Douhéret, Thermochim. Acta **13**, 385 (1975).
[27] C. Moreau and Douhéret, J. Chem. Thermodyn. **8**, 403 (1976).
[28] F. Mato and J. L. Hernandez, An. Quim. **65**, 9 (1969).
[29] M. I. Davis, Thermochim. Acta **63**, 67 (1983).
[30] A. J. Easteal, Aust. J. Chem. **33**, 1667 (1980).
[31] M. I. Davis, Thermochim. Acta **73**, 149 (1984).
[32] C. de Visser, W. J. M. Heuvelsland, L. A. Dunn, and G. Somsen, J. Chem. Soc., Faraday Trans. **74**, 1159 (1978).
[33] E. Matteoli and L. Lepori, J. Chem. Phys. **80**, 2856 (1984).
[34] M. I. Davis, Thermochim. Acta **71**, 59 (1983).
[35] M. I. Davis and G. Douhéret, Thermochim. Acta **104**, 203 (1986).
[36] Y. Marcus and Y. Migron, J. Phys. Chem. **95**, 400 (1991).
[37] G. Eaton, A. S. Pena-Nuñez, and M. C. R. Symons, J. Chem. Soc., Faraday Trans. **84**, 2181 (1988).
[38] G. Eaton, A. S. Pena-Nuñez, M. C. R. Symons, M. Ferrario, and I. R. McDonald, J. Chem. Soc., Faraday Trans. **85**, 237 (1988).
[39] D. Jamroz, J. Stangret, and J. Lindgren, J. Am. Chem. Soc. **115**, 6165 (1993).
[40] J. E. Bertie and Z. Lan, J. Phys. Chem. **101**, 4111 (1997).
[41] K. L. Rowlen and J. M. Harris, Anal. Chem. **63**, 964 (1991).
[42] M. Stoev, A. Makarow, and J. M. A. Robledo, Spectrosc. Lett. **28**, 1251 (1995).
[43] E. v. Goldammer and H. G. Hertz, J. Phys. Chem. **74**, 3734 (1970).
[44] J. R. Damewood and R. A. Kumpf, J. Phys. Chem. **91**, 3449 (1987).
[45] P. I. Nagy, Acta Chim. Hungary **129**, 429 (1992).
[46] K. Nakanishi, Chem. Soc. Rev. **X**, 177 (1993).
[47] H. Kovacs and A. Laaksonen, J. Am. Chem. Soc. **113**, 5596 (1991).
[48] E. Hawlicka, Polish J. Chem. **70**, 821 (1996).
[49] H. Kovacs and A. Laaksonen, J. Am. Chem. Soc. **113**, 5596 (1991).
[50] E. Hawlicka, Polish J. Chem. **70**, 821 (1996).
[51] X.-C. Zhang, B. B. Hu, J. T. Darrow, and D. H. Auston, Appl. Phys. Lett. **56**, 1011 (1990); N. Katzenellenbogen and D. Grischkowsky, *ibid.* **58**, 222 (1991).
[52] J. T. Kindt and C. A. Schmuttenmaer, J. Phys. Chem. **100**, 10 373 (1996).
[53] S. R. Keiding, J. Phys. Chem. **101**, 5250 (1997).
[54] C. Rønne, L. Thrane, P. O. Åstrand, A. Wallqvist, K. V. Mikkelsen, and S. R. Keiding, J. Chem. Phys. **107**, 5319 (1997).
[55] B. N. Flanders, R. A. Cheville, D. Grischkowsky, and N. F. Scherer, J. Phys. Chem. **100**, 11824 (1996).
[56] Y. Y. Akhadov, *Dielectric Properties of Binary Solutions* (Pergamon, New York, 1980).
[57] T. Tassaing, Y. Danten, M. Besnard, E. Zoïdis, and J. Yarwood, Chem. Phys. **184**, 225 (1994).
[58] H. Wode and W. Seidel, Ber. Bunsenges. Phys. Chem. **98**, 927 (1994).
[59] P. Turq, J. Barthel, and M. Chemla, *Transport, Relaxation, and Kinetic Processes in Electrolyte Solutions* (Springer-Verlag, New York, 1992).
[60] P. Kedziora, J. Jadzyn, and P. Bonnet, Ber. Bunsenges. Phys. Chem. **97**, 864 (1993).

[61] *Water: A Comprehensive Teatise*, edited by F. Franks, (Plenum, New York, 1972), Vol. 1.
[62] K. Mizoguchi, Y. Hori, and Y. Tominaga, J. Chem. Phys. **97**, 1961 (1992).
[63] G. E. Walrafen, M. S. Hokmabadi, W. H. Yang, Y. C. Chu, and B. Monosmith, J. Phys. Chem. **93**, 2909 (1989).
[64] H. R. Zelsmann, J. Mol. Struct. **350**, 95 (1995).
[65] U. Kaatze, J. Chem. Eng. Data **34**, 371 (1989).